

Impurity-Induced Optical Fluorescence in MnF_2 †

R. L. GREENE AND D. D. SELL*

Department of Physics, Stanford University, Stanford, California

AND

R. S. FEIGELSON

Center for Materials Research, Stanford University, Stanford, California

AND

G. F. IMBUSCH‡ AND H. J. GUGGENHEIM

Bell Telephone Laboratories, Murray Hill, New Jersey

(Received 29 December 1967)

The optical fluorescence of nominally pure MnF_2 has been studied at low temperatures. It is found that all of the fluorescence, except the very weak intrinsic fluorescence, is induced by small concentrations of cation impurities in the samples. By selectively doping crystals, the characteristic structure for Mg^{2+} , Zn^{2+} , and Ca^{2+} impurities has been identified. In each case, the fluorescence consists of one or two sharp electronic transitions (exciton lines) shifted to a lower energy relative to the intrinsic exciton line, a magnon sideband associated with each exciton line, and a broad band. The exciton lines are identified by polarization and Zeeman experiments. The magnon sidebands are identified by their positions, shapes, and Zeeman behaviors. Each sideband is associated with a particular exciton line by comparing the temperature-dependent lifetimes and intensities of the individual lines. All of these experiments, especially the lifetime and intensity results, strongly suggest that the fluorescence originates at Mn^{2+} ions which are perturbed by nearby impurity ions. The excited energy level of the perturbed Mn^{2+} ion can be shifted to a lower energy, thereby creating a trap for the freely propagating intrinsic excitons. As a result, the intensities and inverse lifetimes of the fluorescence exhibit an activation behavior; that is, they vary as $e^{\Delta/kT}$, where Δ is the depth of the trap. The data are accounted for quantitatively by this model, and values are obtained for the various parameters that describe the energy transfer between the perturbed and unperturbed ions. Finally, it is shown that this model provides an alternative interpretation for the band shift previously discussed by other workers.

I. INTRODUCTION

ANTIFERROMAGNETIC manganese fluoride exhibits a rather strong optical fluorescence at low temperatures. This fluorescence, which we describe here, is of interest for several reasons. First of all, the absorption spectra of MnF_2 and a number of other antiferromagnetic insulators have been studied in considerable detail.¹ Magnon sidebands and magnon line broadening are two prominent magnetic effects that are seen in most of these materials. Fluorescence studies can provide a valuable complement to the absorption work, but to date there is no extensive literature on the fluorescence of such materials.

The fluorescence from MnF_2 is also of interest because of its strong temperature dependence, which is quite different from that observed for dilute magnetic ions in nonmagnetic hosts. This difference is caused by the strong energy transfer in the concentrated material and is related to the presence of small concentrations of impurities in the crystal. In this respect the fluores-

cence from magnetic crystals is similar to that from semiconductors and molecular crystals.²

Figure 1 shows the emission spectrum of a nominally pure sample of MnF_2 at 2°K and also a portion of the absorption spectrum corresponding to the lowest energy ${}^6A_{1g}({}^6S) \rightarrow {}^4T_{1g}({}^4G)$ electronic transitions of the Mn^{2+} ion. The absorption consists of two magnetic dipole pure electronic transitions, followed at higher energies by electric dipole structure, some of which has been identified as magnon sidebands.³ The fluorescence is characterized by sharp structure, shifted to lower energy from the absorption, followed by broad bands at still lower energy.

We have studied the polarization and dipole characters, the magnetic field behavior, and the temperature dependence of intensities and lifetimes of several of the sharp fluorescent transitions. All of these properties can be described by a model in which the emission originates at Mn^{2+} ions which are perturbed by nearby impurities. The lowest excited level of a Mn^{2+} ion near an impurity has its energy reduced and acts as a trap. These traps are efficiently fed by the main body of unperturbed ions.

We shall not discuss the symmetry of the fluorescing ion and its crystallographic relation to the impurity.

† Work at Stanford supported in part by the National Aeronautics and Space Administration under Grant No. NsG 331 and in part by the Advanced Research Projects Agency through the Stanford Materials Research Center.

* Present address: Bell Telephone Laboratories, Murray Hill, N.J.

‡ Present address: Department of Physics, University College, Galway, Ireland.

¹ Some of this work is discussed in a review by D. D. Sell, *J. Appl. Phys.* **39**, 1030 (1968).

² A review of the fluorescence from molecular crystals is given by A. S. Davydov, *Usp. Fiz. Nauk* **82**, 393 (1964) [English transl.: *Soviet Phys.—Usp.* **7**, 145 (1964)].

³ D. D. Sell, R. L. Greene, and R. M. White, *Phys. Rev.* **158**, 489 (1967); and references therein.

Although this is an interesting question, it is not vital to our discussion. We identify certain sharp structure as magnon sidebands, but no attempt is made to analyze their shapes or selection rules. These points will be discussed elsewhere. Dietz and co-workers⁴ have shown that there is also a very weak intrinsic fluorescence from unperturbed Mn^{2+} ions. This will not be dealt with here.

Portions of this work have been presented elsewhere.⁵⁻⁸ Other workers⁹ have studied the broad band fluorescence from MnF_2 for temperatures above 20°K and have interpreted their results on the basis of a model which is at variance with ours.

We are primarily interested in the sharp fluorescence structure which is shown more clearly in Fig. 2. Traces (a), (b), and (c) show the spectra of three different nominally pure crystals at 2°K . The differences in the spectra suggest that the impurities are important. On the other hand, the general similarities in the spectra and their proximity to, and near symmetry with, the absorption band suggest that the fluorescence originates at Mn^{2+} ions rather than at impurity ions. To determine the role of the impurities, crystals were doped with specific impurities. Traces (d), (e), and (f) in Fig. 2 show the spectra for crystals with 0.17% Zn^{2+} , 0.10% Mg^{2+} , and 0.10% Ca^{2+} , respectively. A careful compari-

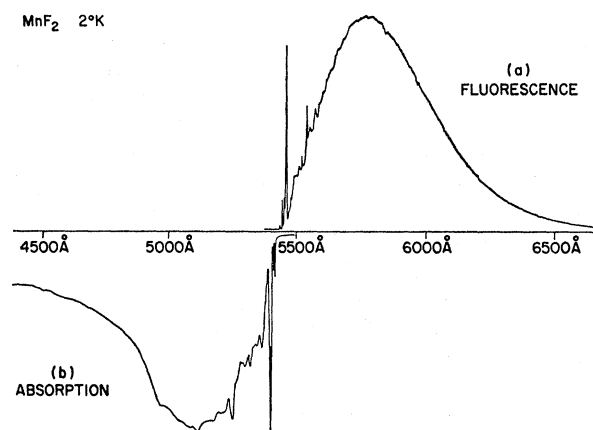


FIG. 1. The fluorescence spectrum of MnF_2 at 2°K and a portion of the absorption spectrum corresponding to transitions from ${}^6A_{1g}$ to the lowest ${}^4T_{1g}$ state.

⁴ R. E. Dietz, H. J. Guggenheim, and A. Missetich, *Bull. Am. Phys. Soc.* **12**, 283 (1967); R. E. Dietz, A. Missetich, A. E. Meixner, and H. J. Guggenheim (to be published).

⁵ D. D. Sell, R. L. Greene, W. M. Yen, A. L. Schawlow, and R. M. White, *J. Appl. Phys.* **37**, 1229 (1966).

⁶ D. D. Sell, R. L. Greene, and A. L. Schawlow, *Bull. Am. Phys. Soc.* **11**, 243 (1966).

⁷ R. L. Greene, D. D. Sell, and R. M. White, in *Optical Properties of Ions in Crystals*, edited by H. M. Crosswhite and H. W. Moos (Interscience Publishers, Inc., New York, 1967).

⁸ R. L. Greene, Ph.D. thesis, Stanford University, Stanford, Calif., 1967 (unpublished).

⁹ W. W. Holloway, Jr., E. W. Prohofskey, and M. Kestigian, *Phys. Rev.* **139**, A954 (1965); and references to their earlier work therein.

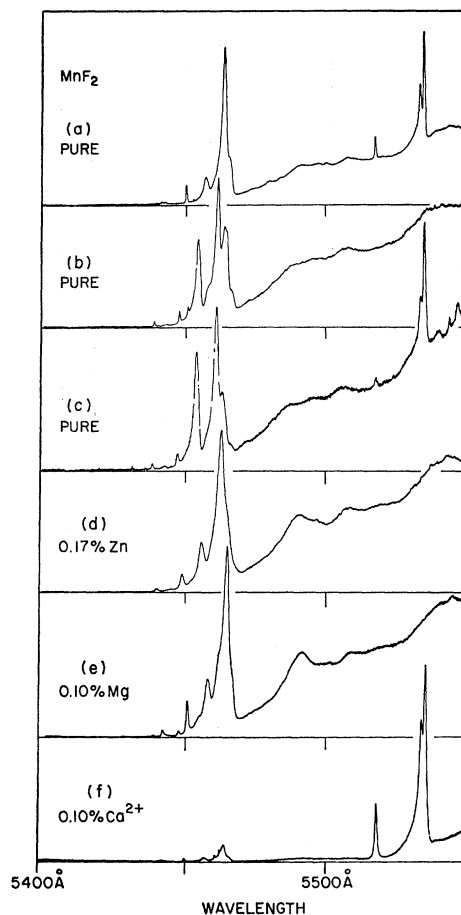


FIG. 2. The sharp-line fluorescence from several samples of MnF_2 at 2°K . Traces (a), (b), and (c) are for nominally pure samples. The samples for traces (d), (e), and (f) were purposely doped as indicated. The intensity scales are not the same for the different traces.

son of these spectra, together with the results discussed in the following sections, leads us to conclude that each of these impurities induces a characteristic fluorescence structure. The four-line structure in the $5450\text{-}\text{\AA}$ region of Fig. 2(a) shown in more detail in Fig. 3(a) is characteristic of MnF_2 with Mg^{2+} impurities. A similar structure displaced toward higher energies by approximately 10 cm^{-1} results for Zn^{2+} impurities. The structure in the $5525\text{-}\text{\AA}$ region of Fig. 2(a) which is shown more clearly in Fig. 3(b), is associated with Ca^{2+} impurities. It is found that a few parts per million of an impurity is sufficient to cause an easily observable effect. Since most of the crystals presently available contain impurities in such concentrations, they exhibit the spectra characteristic to the impurities. It is found that the total fluorescent intensity is relatively insensitive to the total impurity content (as long as no quenching traps are purposely introduced) and that the relative intensity of the characteristic fluorescence of different types of impurities in a crystal scales approximately

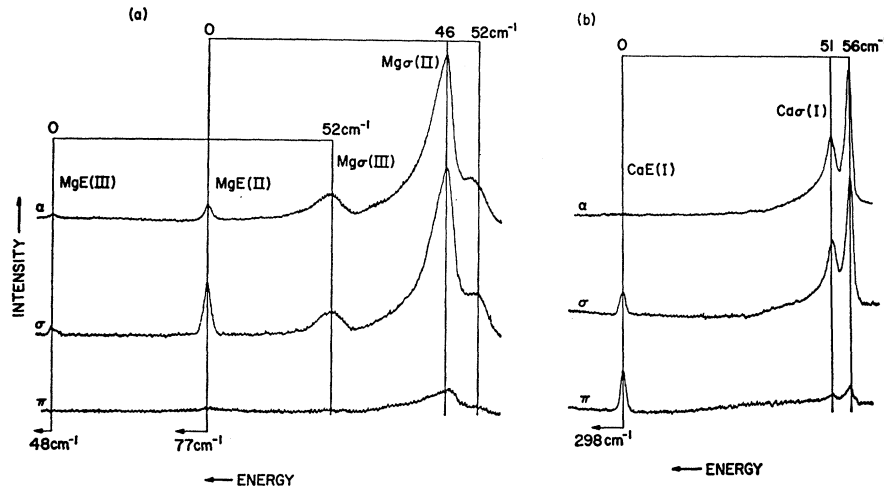


FIG. 3. The sharp structure associated with (a) Mg^{2+} and (b) Ca^{2+} impurities. The traces correspond to α , σ , and π polarization as shown. The numbers above the traces indicate the energy separations of the sideband peaks from the respective electronic transitions. The numbers below the traces indicate the energy separation of the respective electronic lines from the intrinsic exciton line $E(I)$.

as the ratio of the concentrations of the various impurities.

The identification of the structure caused by Zn^{2+} and Ca^{2+} is rather unambiguous. However, it is found that other impurities in addition to Mg^{2+} lead to structure very similar to that shown in Fig. 3(a). We cannot rule out the possibility that the structure which we ascribe to Mg may be associated with one of these other impurities.¹⁰

Our notation is indicated in Fig. 3. The symbol for a transition indicates the impurity involved. For an electronic transition, the symbol contains an E . For a sideband it contains either a σ or a π to denote the polarization in which the transition is seen. The Roman numeral in parentheses denotes the crystallographic relation of the fluorescing ion to the impurity. The cases I, II, and III, respectively, indicate that the impurity is a first, second, or third neighbor of the fluorescing ion. Thus, for example, $\text{Mg}E(\text{II})$ is the electronic transition caused by a second-neighbor Mg^{2+} ion. The transition $\text{Mg}\sigma(\text{II})$ is the σ -polarized magnon sideband of this transition. The experimental evidence which leads us to make the line assignments shown in Fig. 3 is discussed in the following sections. (The crystallographic relation of the impurity to the fluorescing ion follows from our symmetry considerations discussed in Ref. 8 and also from the sideband line-shape calculations of Missetich *et al.*¹¹ These results will be discussed in more detail elsewhere.)

A shorthand notation is also used in the following sections. A symbol such as $\text{Mg}(\text{II})$ is used to denote all of the structure arising from a second-neighbor Mg impurity. The shortened symbol E or σ is used when all the perturbed excitons or all the sidebands are discussed collectively.

¹⁰ R. E. Dietz has also studied crystals doped with various impurities. His results tend to support the assignments given here.

¹¹ A. Missetich, R. E. Dietz, and H. J. Guggenheim, in *Localized Excitations in Solids*, edited by R. F. Wallis (Plenum Press, Inc., New York, 1968).

Finally, we should note that the impurity-induced electronic transitions are quite similar to the lowest-lying intrinsic exciton line denoted as $E1$ in the literature. It will be seen, in fact, that line $E1$ plays an important role in the description of the fluorescence. Thus, it is natural to refer to lines such as $\text{Mg}E(\text{II})$ as perturbed exciton or localized exciton transitions.

II. EXPERIMENTAL DETAILS

The spectra were analyzed with a $\frac{3}{4}$ -m (Spex 1700) and a 1-m (Jarrell-Ash 78-460) Czerny-Turner scanning spectrometer used in first order. The instrumental linewidth was typically 0.5 cm^{-1} . For the lifetime experiments, a xenon flash lamp (PEK XE1-1) was used to excite the fluorescence. With 100-J input energy, the lamp produced a critically damped pulse of 100- to 300- μsec duration, for the properly chosen circuit parameters.¹² The signal was detected by a photomultiplier (EMI-9558Q), integrated to improve the signal-to-noise ratio, logarithmically amplified, and displayed with an oscilloscope (Tektronix 547). Thus, exponentially decaying signals yielded linear oscilloscope traces. The lifetimes were determined by measuring the slopes of these traces. This data processing facilitated data reduction, reduced the errors, and allowed signals with more than one lifetime to be easily recognized. Lifetimes from approximately 0.5 to 38 msec were measured. The error varied from approximately $\pm 3\%$ for the longer lifetime to $\pm 10\%$ for the shortest ones.

For studies other than the lifetime experiments, the fluorescence was excited by a 1000-W, high-pressure, water-cooled mercury arc lamp (General Electric AH-6) with a copper sulfate filter. The signal was detected with a photomultiplier, amplified, and recorded in the usual manner.

In all cases a Corning 7-59 filter was used to filter

¹² J. P. Markiewicz and J. L. Emmett, *IEEE J. Quantum Electron.* **QE-2**, 707 (1966).

the pump light, and a Corning 3-71 filter was used at the spectrometer entrance slit.

Sample temperatures between 4.2 and 77°K were obtained by boiling liquid helium in a storage Dewar and blowing the cold helium gas over the sample. Stable temperatures ($\pm 0.2^\circ K$) were maintained for over ten minutes by controlling the electrical power used to boil the helium and/or controlling the electrical power supplied to a resistor attached to the copper sample holder. The lowest temperature obtained by this method was 4.8°K. For temperatures below 4.2°K the sample was immersed in liquid helium.

Temperatures were measured by monitoring the resistance of a carbon resistor with an ac bridge. Whenever possible, the temperature sensing element was glued to the sample with General Electric 7031 varnish. Different resistors were used above and below 20°K. Below 20°K the temperatures could be read accurately to $\pm 0.1^\circ K$; above 20°K to $\pm 0.2^\circ K$. For temperatures above 15°K a copper versus gold-cobalt thermocouple was used as an additional check on the temperatures. The resistors were calibrated by immersing them in liquid helium, liquid hydrogen, and liquid nitrogen,

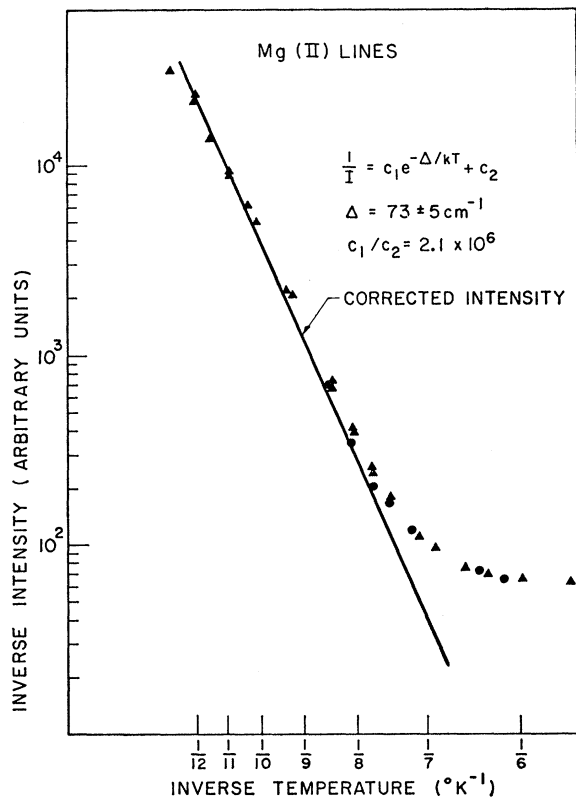


FIG. 4. The inverse intensity of the Mg(II) lines as a function of inverse temperature. The solid triangles and circles represent the data for lines $Mg\sigma$ (II) and MgE (II), respectively. The corrected intensity curve is obtained by subtracting the inverse intensity at very low temperatures (c_2) from the inverse intensity at a given temperature.

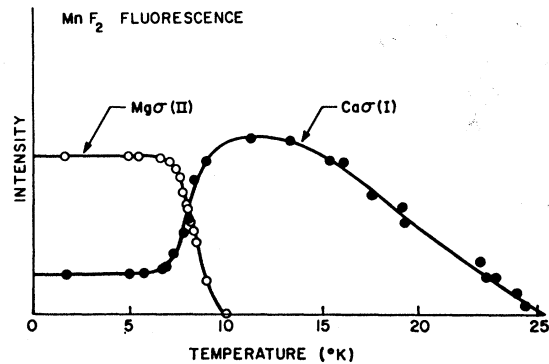


FIG. 5. The intensities of lines $Mg\sigma$ (II) and $Ca\sigma$ (I) as a function of temperature.

using the temperature-versus-vapor-pressure curves to get the correct boiling temperatures, and then using the empirical formula given by White.¹³ It was found that in the region of 10°K, an important region for these experiments, the resistance-versus-temperature calibration could be varied by a few tenths of a degree by using different calibration points. This can lead to a systematic error in the value of Δ obtained below. Also, there was evidence that the sample temperature tended to be a fraction of a degree higher than the sample mounting block and the temperature sensing resistor. This could cause a further systematic error in Δ .

The samples of MnF_2 were grown by the modified Bridgman technique described previously.³ Most samples were spectrographically analyzed to determine the impurity content. The sample with the spectrum shown in Fig. 2(a), for example, contained approximately 10 ppm of Ni, Ca, Fe, Al, Mg, and smaller concentrations of V, Zn, and Co.

Oriented samples were used for the polarization studies. The polarizer and sample were aligned by using the sample as a wave plate between a pair of crossed polarizers and shining a beam of light through these elements just as one would do for an absorption experiment. The leakage of the unwanted polarization could not be measured directly, but it appears that the polarization discrimination was approximately 20 to 1.

Magnetic fields up to 17 kOe were obtained with a 12-in. Varian magnet. Large continuous fields up to 81 kOe were obtained with a Bitter magnet.

III. RESULTS

A. Polarizations

The polarization results are shown in Fig. 3 for the Mg- and Ca-induced lines. The results for the Zn impurities are very similar to the Mg results shown in Fig. 3(a). The dipole character of the lines is determined by comparing the $\alpha(\mathcal{E} \perp c, \mathcal{I} \perp c)$ polarization

¹³ G. K. White, *Experimental Techniques in Low-Temperature Physics* (Clarendon Press, Oxford, England, 1959), Chap. 4.

with $\sigma(\mathbf{E} \perp c, \mathcal{H} \parallel c)$ and $\pi(\mathbf{E} \parallel c, \mathcal{H} \perp c)$ to see whether the electric or magnetic vector causes the transition. It is seen that the E lines have both electric and magnetic dipole character. For $\text{Mg}E(\text{II})$ and also $\text{Zn}E(\text{II})$ the ratio of the electric to magnetic dipole character is approximately 1 to 4. For $\text{Ca}E(\text{I})$, the electric to magnetic dipole ratio is approximately 2 to 1.

These are the results one expects for pure electronic transitions near an impurity. An unperturbed Mn^{2+} ion is at a center of symmetry in MnF_2 . It can only undergo magnetic dipole pure electronic transitions. However, the effect of a nearby impurity can destroy the inversion symmetry for its neighboring ions (in general, it lowers the site symmetry). Thus electric dipole transitions are permitted due to the small amount of "oddness" introduced into the predominantly even electronic states.

There appears to be a correlation between the ratio of the electric to magnetic dipole transition strength and the energy shift of a line from its unperturbed energy. Line $\text{Ca}E(\text{I})$, which is 298 cm^{-1} from the lowest-energy electronic transition (line $E1$) seen in absorption, has more electric dipole character than line $\text{Mg}E(\text{II})$, which is only displaced 77 cm^{-1} . This is reasonable since both of these properties (energy shift and oddness) might be expected to depend upon the strength of the perturbation which the impurity causes at the fluorescing ion.

It was assumed that the transitions assigned as magnon sidebands are pure electric dipole transitions, as they are in the absorption spectrum. This information was then used to normalize the α traces in Fig. 3 such that the sidebands have the same intensities in σ and α polarizations. This was necessary because a different sample was used for α polarization than was used for σ and π . These transitions have properties characteristic of magnon sidebands. They are very strongly polarized as are the sidebands seen in absorption and their peaks are separated by approximately 50 cm^{-1} (a typical zone-boundary magnon energy) from their respective electronic transitions. We do not attempt to make complete use of this line-shape data here, but it is noteworthy that the profile of $\text{Ca}\sigma(\text{I})$ mirrors almost exactly the magnon density of states [for the zero of magnon energy at line $\text{Ca}E(\text{I})$]. Further proof that the σ lines are magnon sidebands is discussed below.

B. Magnetic Field Behavior

In a 17-kOe magnetic field applied parallel to the z axis, the E lines split into two equal-intensity components which are symmetrically displaced from the zero-field position. In each case the splitting is approximately 2.9 cm^{-1} . The electric dipole σ transitions do not split and no broadening caused by unresolved splitting is observed. None of the lines split when the field is applied perpendicular to the z axis.

These results are essentially the same as those observed for the absorption transition to this same ${}^4T_{1g}$ excited state. The theory for the absorption case is thoroughly discussed in Refs. 3 and 5. We shall only review the results here. The pure electronic absorption transitions $E1$ and $E2$ are spin-forbidden transitions in which the z component of spin changes by $+1$ for one sublattice and -1 for the other. In a magnetic field the transition energy increases for ions on one sublattice and decreases for ions on the other sublattice. The observed splitting is

$$\Delta_1 = 2\beta H_0 |gS - g'(S-1)|, \quad (1)$$

where the g values in the ground and excited states are g and g' , respectively, and S is the spin in the ground state. For MnF_2 , $g=2.00$ and $S=\frac{5}{2}$. From the observed splitting it was found that the excited states for $E1$ and $E2$ have $g'=2.11$. The fact that the E lines all exhibit the same behavior and have a $g' \approx 2.1$ is further strong evidence that these lines are exciton transitions.

The sideband transitions in absorption ($\sigma 1$, $\pi 1$, and $\sigma 2$ of Ref. 3) are transitions in which the total z component of spin for the crystal does not change. For these transitions the spin flip of the exciton which is on one sublattice cancels the spin flip of the magnon which is predominantly on the opposite sublattice. For the general case, the splitting should be

$$\Delta = 2\beta H_0 (S-1) |g' - g|, \quad (2)$$

but since $g' \approx g$ no splitting is observed.

This absence of splitting applies for sidebands in emission as well if one modification is made. For emission, in order to conserve the total z component of spin, the magnon and the exciton should be on the same sublattice (or on opposite sublattices if zero-point deviations are involved). The fact that no splitting is observed in the σ fluorescence transitions strongly supports their identification as sidebands.

The absence of any splitting of the fluorescence spectrum in a field perpendicular to the z axis is similarly accounted for by the theory for the absorption case. In an attempt to see any small splitting or broadening of the sidebands a field of 81 kOe was applied parallel to the z axis. No such effects were found to within an accuracy of 0.5 cm^{-1} .

C. Temperature Dependence of Intensities

The fluorescent intensity exhibits an interesting temperature dependence. All of the structure shown in Figs. 2 and 3 is observed at temperatures below 4.2°K . Within approximately a $\frac{1}{2}^\circ$ temperature span near 4.8°K the $E(\text{III})$ and $\sigma(\text{III})$ lines for Mg and Zn lose their intensity rapidly and become unobservable. This is a difficult temperature region in which to work. Consequently, the temperature dependence of these lines was not studied quantitatively.

Near $10^\circ K$, lines $E(II)$ and $\sigma(II)$ for Mg and Zn undergo a similar behavior. The variation of the intensity as a function of temperature is shown in Fig. 4 for lines $MgE(II)$ and $Mg\sigma(II)$. These data were taken on the sample with the spectrum shown in Fig. 2(a). Similar results were observed in other samples, but this sample proved to be a particularly simple one to study since it has predominantly Mg and Ca induced fluorescence and these two sets of lines are well separated in energy. The more accurate data could be obtained for the stronger transition $Mg\sigma(II)$, but it is clear that both lines have the same temperature dependence. In previous sections we have shown that $Mg\sigma(II)$ is a sideband. The data on its temperature dependence confirms that it is a sideband of line $MgE(II)$. In a similar way, it is found that the intensities and also the lifetimes of all of the sidebands which we discuss have the same temperature-dependent behavior as their respective electronic transitions.

It is seen from Fig. 4 that for sufficiently high temperature the intensity has an exponential behavior. This is discussed more fully in Sec. IV. It is shown that the observed exponential temperature dependence results from an activation process in which the activation energy is simply the difference in energy between the lowest levels of the perturbed and unperturbed Mn^{2+} ions. This energy is denoted by Δ .

It was found that the intensity, or at least some of the intensity, lost by the $Mg(II)$ system was gained by the Ca impurity-induced lines. This was studied

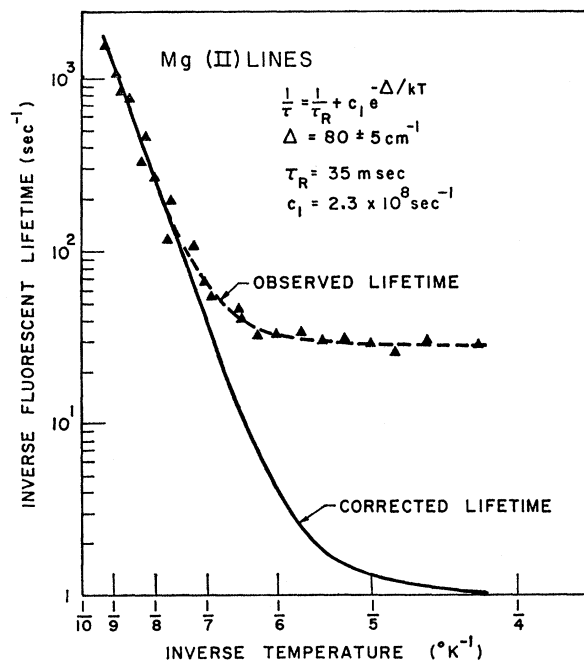


FIG. 6. The inverse fluorescent lifetime of the $Mg(II)$ lines as a function of inverse temperature. The corrected lifetime is obtained from the data by subtracting the inverse of 35 msec (τ_R) from the inverse lifetime.

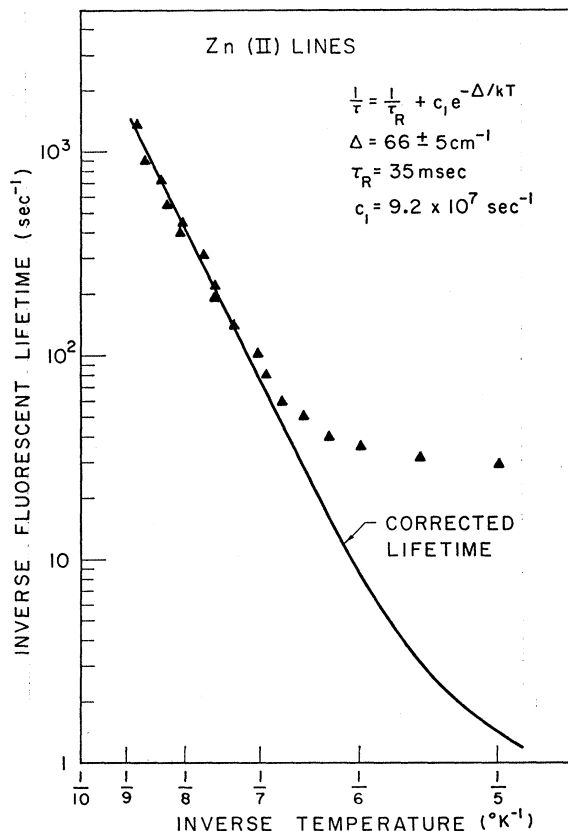


FIG. 7. The inverse fluorescent lifetime of the $Zn(II)$ lines as a function of inverse temperature.

quantitatively in the sample with the spectrum shown in Fig. 2(a). The results are shown in Fig. 5 in which the intensities of lines $Mg\sigma(II)$ and $Ca\sigma(I)$ are plotted as a function of temperature. This indicates that the excitation is transferred in some manner from a Mn ion near a Mg ion to a Mn near some Ca ion. It is believed that this energy transfer takes place through the intrinsic excitons. This is discussed further in Sec. IV.

It is found that the total integrated intensity of the optical fluorescence decreases by approximately 15% in this $10^\circ K$ temperature range. This indicates that the excitation lost by the Mg perturbed ions is not transferred completely to other fluorescing centers, but that instead some portion of this excitation is lost to nonradiative centers (or centers which radiate in some other spectral region).

Finally, in the region near $28^\circ K$ the Ca-induced fluorescence begins to exhibit the same decrease in intensity which was seen in the other systems at lower temperatures.

It should be noted that it is also possible to see changes in the broad band fluorescence shown in Fig. 1 which are correlated with the changes discussed above. It appears that this broad band, which is attributed to

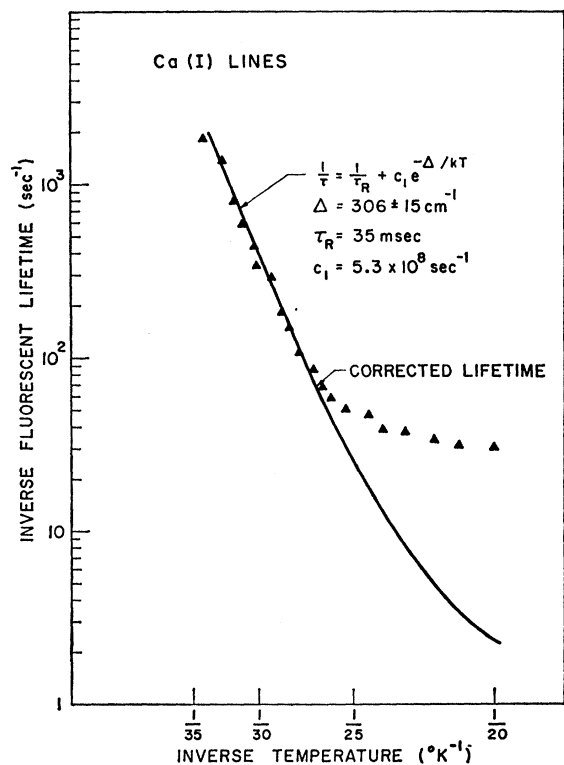


FIG. 8. The inverse fluorescent lifetime of the Ca(I) lines as a function of inverse temperature.

phonon (or possibly phonon plus magnon) assisted transitions, is a composite of separate bands for each of the types of impurity centers. It is seen, for example, that the Ca-induced lines in Fig. 2 are on a broad background which we find has the same temperature dependence as the Mg and Zn induced sharp structure. Thus, as the temperature is increased it is found that the peak of the broad band tends to move toward longer wavelengths. Similar results have been reported previously by Holloway *et al.*,⁹ who have given these results a rather different interpretation than we do here. This is discussed further in Sec. V.

D. Temperature Dependence of Lifetimes

The temperature dependence of the fluorescent lifetimes is similar to that of the intensities discussed above. This is to be expected. Under continuous optical pumping, the intensity at a given frequency is determined by N/τ_R , where N is the number of excited ions with the appropriate energy and τ_R is the spontaneous radiative lifetime. It is reasonable to assume that τ_R is rather insensitive to temperature in the region of interest and that the temperature dependence of the intensity arises from the temperature dependence of N . In a simple situation, N is proportional to the total lifetime of the fluorescing state. Thus a change in the lifetime should have an effect upon the intensity.

At 4.2°K all of the fluorescence, except MgE(III) and Mgσ(III) [and presumably also the corresponding Zn(III) lines, which were not studied thoroughly], has a lifetime of 35 ± 1 msec. Lines MgE(III) and Mgσ(III) have a lifetime of approximately 25 msec. Generally speaking, at a given temperature, the relative intensities of the various lines in these pulse experiments are the same as those observed with continuous excitation. Thus, near 4.8°K, lines MgE(III) and Mgσ(III) become very weak. As this occurs the lifetimes also become much shorter.

The temperature-dependent lifetimes of the E(II) and σ(II) transitions for Mg and Zn and the E(I) and σ(I) transitions for Ca have been studied in detail. The results are shown in Figs. 6-8, respectively. It is seen that the lifetimes exhibit an exponential behavior at sufficiently high temperatures similar to that observed in the intensity experiments, i.e., a decrease in lifetime exponential in $1/T$.

IV. MODEL FOR THE FLUORESCENCE

The results presented above lead us to adopt a model for the fluorescence in which the fluorescence originates at Mn^{2+} ions near impurity ions. It is found that this model gives a thorough quantitative account of the observations. Essentially this same model has been used by Dietz and co-workers¹⁴ to qualitatively describe the impurity-induced fluorescence of other antiferromagnetic insulators. A very similar model has been used to discuss the fluorescence from molecular crystals.²

This model is shown schematically in Fig. 9. The energy levels of Mn^{2+} ions near an impurity ion are perturbed. We are particularly interested in those levels which have a lower energy than the intrinsic exciton

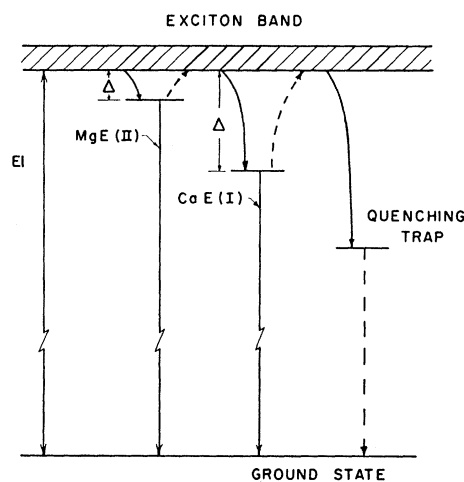


FIG. 9. Schematic representation of fluorescence from MnF_2 .

¹⁴ R. E. Dietz, L. F. Johnson, and H. J. Guggenheim, in *Physics of Quantum Electronics*, edited by P. L. Kelley, B. Lax, and P. E. Tannenwald (McGraw-Hill Book Co., New York, 1966).

band since such levels can trap the excitation at low temperatures.¹⁵ Each perturbed Mn^{2+} ion which has a distinct relation to an impurity has a characteristic energy. One impurity may give rise to several depressed energy levels corresponding, for example, to first-neighbor Mn^{2+} ions, second neighbors (there are two types), etc.

The majority of the Mn^{2+} ions are not perturbed. These ions form the exciton band which has been studied in the absorption work. The very weak fluorescence from these intrinsic excitons has also been studied by Dietz *et al.*⁴

The trapped levels are fed by energy transfer from the intrinsic exciton bands. Only those traps whose lowest excited levels are separated from the intrinsic exciton band by an energy large compared to kT will be stable against thermal scattering back into the intrinsic exciton band. In other words, as the temperature is increased a trapped exciton can be excited up to the intrinsic exciton band by absorbing a thermal phonon (or magnon in some cases). The intrinsic exciton can then propagate to another trap. Since the "boil off" from the trapped levels depends upon a thermal population factor, it should exhibit an activation behavior. In addition, as the temperature increases the intensity of the fluorescence should shift from the shallow traps to the deeper, more stable traps and the total intensity should decrease because of the feeding of quenching traps.

It is important to note that the Mg^{2+} , Zn^{2+} , and Ca^{2+} ions themselves do not have any excited electronic states that lie below the Mn^{2+} exciton band. Thus these impurities cannot trap the excitation directly. There are ions such as Ni^{2+} , for example, which do have lower-lying levels which can act as traps. It has been shown¹⁶ that Ni^{2+} in concentrations on the order of 10 ppm can quench the Mn^{2+} fluorescence quite efficiently. We refer to traps of this type which do not lead to fluorescence in the spectral region of interest (Ni^{2+} fluoresces at approximately 1.5μ) as quenching traps.

In order to make our discussion quantitative, we describe the excitation transfer between the various levels in terms of transition rates and set up rate equations. This is shown schematically in Fig. 10. We consider two levels. Level 1 corresponds to a radiative trap; level 2 to the exciton band. The number of traps and exciton states are g_1 and g_2 , respectively, and the populations in these levels are N_1 and N_2 . The ratio of the number of impurity states to intrinsic states is $n = g_1/g_2$. Typically, n is a number on the order of 10^{-5} .

For the purposes of determining the transition rates

¹⁵ We do not attempt to give a criterion for the appearance of localized excitons in MnF_2 . This problem has not yet been solved for magnetic insulators although it has been discussed for the closely related case of molecular crystals. [See, for example, S. Takeno, *J. Chem. Phys.* **44**, 853 (1966); V. I. Sugakov, *Opt. i Spektroskopiya* **21**, 574 (1966) [English transl.: *Opt. Spectry.* **21**, 319 (1966)].

¹⁶ L. F. Johnson, R. E. Dietz, and H. J. Guggenheim, *Phys. Rev. Letters* **17**, 13 (1966).

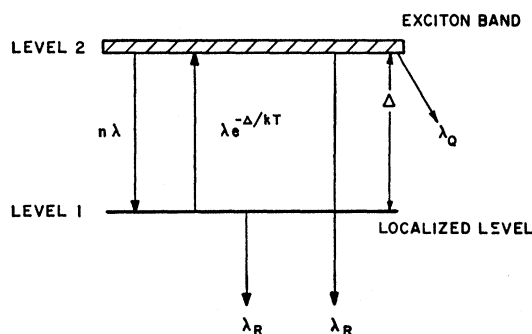


FIG. 10. Schematic representation of the model for impurity-induced fluorescence. The total number of states in the crystal for levels 1 and 2 are g_1 and g_2 , respectively. The ratio $g_1/g_2 = n$ is the concentration of impurities associated with level 1.

between levels 1 and 2, it makes no difference whether we assume that the exciton diffuses from site to site or whether we think of it as spread throughout the crystal. Consider the case in which the exciton is momentarily at a given ion site near a trap. There is a certain transition probability that the exciton will "fall into" the trap and that a phonon (or magnon) will be created to conserve energy. We define λ as the sum of the transition rates for transitions from each of the neighbors to the traps. For an exciton instantaneously at any site, the probability that a specific neighbor is a trap is n , the concentration of traps. Consequently, the total transition rate (probability per unit time) for an exciton in level 2 to undergo a transition to level 1 is $n\lambda$.

The inverse transitions from level 1 to level 2 require thermal phonons (or magnons). For the present problem in which Δ , the energy separation between the two levels, is large compared to kT , this introduces a factor $e^{-\Delta/kT}$. Thus, the total transition rate for transitions from a trap to the exciton band is $\lambda e^{-\Delta/kT}$.

In order to make our discussion more transparent, we make the following plausible assumptions: (1) The radiative transition probability λ_R is the same for the perturbed and unperturbed ions. (2) The radiative traps cannot lose their energy directly to the quenching traps. (3) The traps for the various impurities can be considered independently. (4) The excitation which is trapped at quenching traps is irretrievably lost from the system.

The transition rate from level 2 to the quenching traps is denoted by λ_Q . This includes quenching by Ni^{2+} ions as well as any other quenching centers which may exist. It should be kept in mind that λ_Q , as it has been defined, is directly proportional to the concentration of quenching traps, and thus can vary from crystal to crystal. [For transitions from level 2 to level 1 this has been included explicitly in the factor n ; thus, λ is independent of impurity concentration.]

The work of Dietz *et al.*⁴ on the intrinsic fluorescence (level 2) at low temperatures allows us to estimate the magnitudes of $n\lambda$ and λ_Q . They find that for typical pure

crystals: (1) The impurity-induced fluorescence is about one hundred times as intense as the intrinsic fluorescence. (2) The intrinsic lifetime is approximately 280 μsec . This is to be compared with the impurity-induced lifetime at low temperatures which is 35 msec. (3) The fluorescence from the Ni^{2+} ions (in infrared) is approximately one-tenth that of the optical fluorescing traps.

At low temperatures (below 4.2°K) the upward transitions can be neglected. We can assume that the fluorescing traps gain most of their excitation by transfer from the exciton band. In this case, if we use the fact that the population in a state is equal to the pumping rate times the lifetime, we obtain

$$N_2/N_1 = \lambda_R/n\lambda. \quad (3)$$

Since the intensity from levels 1 and 2 is simply given by $N_1\lambda_R$ and $N_2\lambda_R$, respectively, it can be inferred from point 1 above that

$$n\lambda \approx 100\lambda_R. \quad (4)$$

Similarly, if the Ni^{2+} ions are excited through the transition rate λ_Q , it can be inferred from point 3 that

$$\lambda_Q \approx 10\lambda_R. \quad (5)$$

At low temperatures the ratio of the lifetimes of levels 2 and 1, τ_2/τ_1 is given by

$$\tau_2/\tau_1 = \lambda_R/(n\lambda + \lambda_Q + \lambda_R). \quad (6)$$

Thus Eq. (6) and point 2 are consistent with Eqs. (4) and (5).

The rate equations have the form

$$\begin{aligned} dN_1/dt &= a_{11}N_1 + a_{12}N_2 + g_1\sigma_1F, \\ dN_2/dt &= a_{21}N_1 + a_{22}N_2 + g_2\sigma_2F, \end{aligned} \quad (7)$$

where

$$\begin{aligned} a_{11} &= -(\lambda e^{-\Delta/kT} + \lambda_R), \\ a_{12} &= n\lambda, \\ a_{21} &= \lambda e^{-\Delta/kT}, \\ a_{22} &= -(n\lambda + \lambda_Q + \lambda_R). \end{aligned} \quad (8)$$

F is the flux from the exciting lamp and $\sigma_1(\sigma_2)$ is the excitation cross section for an unperturbed (perturbed) ion.

For the case of time-independent, continuous fluorescence, $dN_1/dt = dN_2/dt = 0$. From Eqs. (7) and (8) we find that

$$N_1 = (c_1 e^{-\Delta/kT} + c_2)^{-1}, \quad (9)$$

where

$$\frac{c_1}{c_2} = \frac{\lambda(\lambda_Q + \lambda_R)}{\lambda_R(n\lambda + \lambda_Q + \lambda_R)}. \quad (10)$$

It is seen by comparing Eqs. (9) and (10) with the data in Fig. 4 that there is good agreement between the

calculated and observed behavior. The important point is that an exponential behavior is observed over a wide range of intensities and the parameter Δ has approximately the expected value. The observed value of $\Delta = 73 \pm 5 \text{ cm}^{-1}$ is in good agreement with the measured separation of 77 cm^{-1} between lines $E1$ and $\text{Mg}E(\text{II})$. The error limits here do not include possible systematic errors. As we have already mentioned in Sec. II, systematic errors could arise from temperature calibration, or from heating of the sample by the pump light. Either of these could cause the recorded temperature to be consistently a few tenths of a degree higher than the actual temperatures. This would cause the measured Δ to be a few wave numbers smaller than the actual Δ . However, the rather good agreement that we obtain here as well as in the lifetime experiments suggests that such systematic errors are quite small.

We can also use the observed value of c_1/c_2 to estimate the Mg-impurity concentration. For the crystal used to obtain the data in Fig. 4 [spectrum shown in Fig. 2(a)], $n\lambda/\lambda_R$ is 40. If we assume that Eq. (5) is approximately correct and substitute these values into Eq. (10) we obtain an impurity concentration of approximately 5 ppm. This is a reasonable value.

To obtain calculated lifetimes, we use Eq. (7) with F set equal to zero. We look for a general solution of the form

$$N_i(t) = A_i e^{m_+ t} + B_i e^{m_- t}, \quad i=1, 2 \quad (11)$$

where

$$m_{\pm} = \frac{1}{2}(a_{11} + a_{22}) \pm \left[\frac{1}{4}(a_{11} + a_{22})^2 - a_{11}a_{22} + a_{12}a_{21} \right]^{1/2}, \quad (12)$$

and the coefficients A and B are related by

$$\begin{aligned} A_2 &= [(m_+ - a_{11})/a_{12}]A_1, \\ B_2 &= [(m_- - a_{11})/a_{12}]B_1. \end{aligned} \quad (13)$$

Thus, using Eq. (8) in Eq. (12),

$$m_{\pm} = -\frac{1}{2}m_0 \pm \frac{1}{2}m_0 \left[1 - 4(\lambda_R m_0 + \lambda_Q \lambda e^{-\Delta/kT})/m_0^2 \right]^{1/2}, \quad (14)$$

where

$$m_0 = n\lambda + \lambda e^{-\Delta/kT} + \lambda_Q + 2\lambda_R. \quad (15)$$

The quantity m_0 , the sum of all the transition rates, appears frequently in the analysis of the lifetimes. Since λ_R is small compared to $n\lambda$ and λ_Q , we can for simplicity neglect it in the expression for m_0 .

Since λ_R is small, the second term beneath the radical in Eq. (14) is small compared to one. The last term beneath the radical will be small for conditions in which either λ_Q or $\lambda e^{-\Delta/kT}$ is small compared to m_0 . In light of our experimental results and the foregoing discussion of the transition rates, this is plausible. We make this assumption and expand the square root keeping only the first term in the series. The result is

$$\begin{aligned} m_+ &= -\left(\lambda_R + \frac{\lambda_Q \lambda e^{-\Delta/kT}}{n\lambda + \lambda e^{-\Delta/kT} + \lambda_Q} \right), \\ m_- &= -m_0 = -(n\lambda + \lambda e^{-\Delta/kT} + \lambda_Q). \end{aligned} \quad (16)$$

Finally, expressions for $N_1(t)$ and $N_2(t)$ can be obtained by using Eq. (13) and choosing the appropriate boundary conditions at time $t=0$. It is reasonable to assume that at $t=0$, $N_1(0)=0$ (that is, level 1 receives all of its population from transfer from level 2 and very little excitation directly from the pump light), and $N_2(0)$ is arbitrary.

This leads to

$$N_1(t) = N_2(0) (n\lambda/m_0) (e^{m_+t} - e^{m_-t}), \quad (17)$$

$$N_2(t) = (N_2(0)/m_0) [\lambda e^{-\Delta/kT} e^{m_+t} + (n\lambda + \lambda_Q) e^{m_-t}]. \quad (18)$$

Since m_+ and m_- are negative quantities and since $|m_-|$ is typically large compared to $|m_+|$, we see that N_1 grows initially as $\sim(1 - e^{m_-t})$, while N_2 decreases as $\sim e^{m_-t}$. This occurs because of the decay from level 2 to level 1. This m_- term tends to establish a thermal equilibrium population between levels 1 and 2. After the rapid achievement of this population equilibrium both N_1 and N_2 decay at the slower rate e^{m_+t} , always maintaining the correct population ratio between levels 1 and 2.

These results can now be compared with the data in Figs. 6, 7, and 8. We see from Eq. (16) that the temperature-dependent lifetime which is observed results from the factor $m_0^{-1}\lambda_Q\lambda e^{-\Delta/kT}$. Note that for $\lambda_Q=0$ the lifetime is temperature-independent. In that case, there is no way for excitation to escape from the fluorescing system.

We see from Eq. (16) that at sufficiently low temperatures the λ_R term predominates and the lifetime becomes temperature-independent. Thus the 35-msec lifetime observed at low temperatures is the radiative lifetime. To isolate the temperature dependence of the lifetime, a corrected lifetime is plotted in Figs. 6-8. The corrected lifetime is obtained by subtracting λ_R from the total transition rate (i.e., subtract the inverse of 35 msec from the inverse observed lifetime). It is seen that the corrected lifetime does exhibit an exponential behavior. The Δ 's obtained in these lifetime experiments, namely, 80 ± 5 cm^{-1} for Mg(II), 68 ± 5 cm^{-1} for Zn(II), and 306 ± 15 cm^{-1} for Ca(I) compare favorably with the measured energy separations from line E1 of 77, 67, and 298 cm^{-1} , respectively. This behavior corresponds to the $\lambda_Q\lambda e^{-\Delta/kT}/m_0$ term. Note, however, that at sufficiently high temperatures such that $\lambda e^{-\Delta/kT}$ is the largest factor in m_0 the transition rate should assume the value λ_Q . This behavior should begin to occur for the very shortest lifetimes measured. However, for our experiments, the signal-to-noise ratio deteriorated rapidly in this region and we were not able to confirm this behavior.

From Eq. (16) we see that, after the establishment of a population equilibrium between N_1 and N_2 , the observed lifetime τ should have the form $1/\tau = (1/\tau_R) + c_1 e^{-\Delta/kT}$, where $c_1 = \lambda_Q\lambda/m_0$. For the case of Mg(II) for which the intensity experiments indicated that the Mg-impurity concentration is approximately 5 ppm,

the calculated value of c_1 is 5.7×10^7 sec^{-1} . This is somewhat smaller than the observed value of 2.3×10^8 sec^{-1} .

V. DISCUSSION

Although we have concentrated upon the properties of the sharp structure, we have also observed the characteristics of the broad fluorescence band as a function of temperature. As was mentioned above, the data indicate that the broad fluorescence is a composite of separate (but similar) bands for each type of impurity center. Thus our model for the sharp-line fluorescence also has a bearing on the broad-band results.

Generally speaking, we observe the same behavior for the broad-band fluorescence which has been reported previously by Holloway, Prohofskey, and Kestegian.⁹ One significant difference is that we find that the abrupt temperature-dependent shift of the band peak near 30°K is sample-dependent. We have observed samples which appear to be normal in other respects but which do not exhibit such a shift.

Holloway *et al.* have described their observations in terms of a model which is quite different from the one presented here. They attribute the unusually large separation between the broad absorption and fluorescence band peaks to a Stokes shift which depends upon magnetoelastic coupling. On the other hand, we infer that this results from the fact that the fluorescence originates at traps.

Furthermore, they ascribe the strong temperature-dependent changes near 30°K to the activation of a virtual local magnon mode. We find that this behavior is accounted for by the model discussed in Sec. IV. Holloway *et al.* indicate that the observed temperature dependence is too strong to be accounted for as an activation process. Presumably, they are referring to an activation of the form $e^{-\alpha/T}$, where α is the temperature at which the changes occur. We have seen, however, that since the fluorescence originates from traps, the activation has a form $e^{-\Delta/kT}$, where Δ is much larger than the temperature at which the variations occur. This accounts for strong temperature dependence.

It is believed that the model discussed here should have a rather general applicability to the impurity-induced fluorescence in antiferromagnets. For example, it may have a bearing on the work of Eremenko *et al.* on the fluorescence of MnF_2 doped with Eu^{3+} .¹⁷

VI. SUMMARY

The optical fluorescence of nominally pure MnF_2 has been studied at low temperatures. It is found that all of the fluorescence, except the very weak intrinsic fluorescence, is induced by small concentrations of cation impurities in the samples. By selectively doping

¹⁷ V. Eremenko, E. V. Matyuskin, and S. V. Petrov, Phys. Status Solidi **18**, 683 (1966).

crystals, the characteristic structure for Mg^{2+} , Zn^{2+} , and Ca^{2+} impurities has been identified. In each case, the fluorescence consists of one or two sharp electronic transitions (exciton lines) shifted to lower energy relative to the intrinsic exciton line, a magnon sideband associated with each exciton line, and a broad band.

The exciton lines are identified by polarization and Zeeman experiments. The magnon sidebands are identified by their positions, shapes, and Zeeman behaviors. Each sideband is associated with a particular exciton line by comparing the temperature-dependent lifetimes and intensities of the individual lines.

All of these experiments, especially the lifetime and intensity results, strongly suggest that the fluorescence originates at Mn^{2+} ions which are perturbed by nearby impurity ions. The excited energy level of the perturbed Mn^{2+} ion can be shifted to lower energy, thereby creating a trap for the freely propagating intrinsic excitons. As a result, the intensities and inverse lifetimes of the fluorescence exhibit an activation behavior; that is, they

vary as $e^{\Delta/kT}$, where Δ is the depth of the trap. The data are accounted for quantitatively by this model and values are obtained for the various parameters that describe the energy transfer between the perturbed and unperturbed ions.

Finally, it is shown that this model provides an alternate interpretation for the band shift previously discussed by other workers.

ACKNOWLEDGMENTS

Much of this work was conducted in Professor A. L. Schawlow's laboratory at Stanford University. His stimulation and encouragement have been of particular value to two of us (R. L. G. and D. D. S.). We gratefully acknowledge several helpful discussions with R. E. Dietz and thank him for allowing us to quote his unpublished results. We wish to thank J. P. van der Ziel, who made the Zeeman measurements at high magnetic fields, and M. B. Graifman for experimental assistance.

Errata

Ultrasonic Attenuation of Pure Strong-Coupling Superconductors, JAMES W. F. WOO [Phys. Rev. **155**, 429 (1967)]. An over-all minus sign was missing from the right-hand side of Eq. (3.2). An error was found in the numerical work, so that Fig. 1 is incorrect. The corrected result, as well as an expression for the reduced attenuation valid for all values of ql , will be presented in a future paper.

Quantum Theory of Spontaneous Parametric Scattering of Intense Light, T. G. GIALLORENZI AND C. L. TANG [Phys. Rev. **166**, 225 (1968)]. In the denominator on the right side of Eq. (36), " πC^4 " should read " $2\pi C^4$," and " $n_e^2(\omega_p^{1/2}\pi)$ " should read " $n_e(\omega_p^{1/2}\pi)$."